Manifestation of classical chaos in the statistics of quantum energy levels

Th. Zimmermann, H.-D. Meyer, H. Köppel, and L. S. Cederbaum
Theoretische Chemie, Physikalisch-Chemisches Institut, Universität Heidelberg, Im Neuenheimer Feld 253, D-6900 Heidelberg, West Germany
(Received 3 February 1986)

We investigate the quantum energy-level sequence of two coupled quartic oscillators. The classical system is a scaling one and has been shown elsewhere to undergo a transition from regular to irregular motion for increasing coupling strength. The distribution of spacings between adjacent energy levels $P(S)$ and the Δ_3 statistic indicate a corresponding transition from an uncorrelated spectrum where successive levels arrive randomly to a spectrum described by the Gaussian orthogonal ensemble of random matrices. For $P(S)$ we use Berry and Robnik's semiclassical formulas which depend on the volumes of regions in phase space filled with chaotic trajectories and the extension of this *ansatz* to the Δ_3 statistic. We investigate systematic deviations from this picture due to quantum effects and discuss their universality. We find that $P(S)$ is mainly sensitive to the total irregular fraction of phase space, whereas Δ_3 strongly reflects its partitioning into several parts. For vanishing coupling strength, where the system becomes integrable, we find extremely slow convergence to the semiclassical limit.

I. INTRODUCTION

The phrase "quantum chaos" has by now become very popular. Much work has been dedicated to the problem of how the classically well-defined attributes "regular" and "chaotic" behavior[1] for bound Hamiltonian systems are mirrored in their quantum counterparts, where their definition is less obvious or even meaningless. From the correspondence principle, however, it is clear that there is a connection between classical and quantum systems. Thus there have been several attempts to link certain classical properties with their quantum counterparts, e.g., via the motion of wave packets.[2] Several other indicators for quantum chaos have been proposed, such as correlation properties of wave functions,[3] applicability of semiclassical quantization,[4] or sensitivity of energy levels to perturbations.[5]

While most of these ways try to transfer classical dynamical concepts into the corresponding quantum system, a very fruitful approach to characterize quantal manifestations of regular and chaotic behavior is the inspection of statistical properties of the quantum energy-level sequence.[6] In nuclear physics this point of view has a long tradition, where appropriate random matrix ensembles have been used to describe features of complicated experimental spectra.[7,8] In particular, several useful statistical measures have been introduced, the most important ones being the distribution of energy-level spacings (nearest-neighbor spacings, nns) $P(S)$ and the Δ_3 statistic,[9] measuring short- and long-range correlations of the spectral sequence, respectively. More recently, these methods have also been used in the description of highly complex atomic[10] and molecular[11] spectra.

For a regular,[12] i.e., classically integrable, system it has been proved, for the generic case, that in the semiclassical limit $\hbar \to 0$, successive energy levels arrive randomly, resulting in a Poisson distribution for $P(S)$.[13] For generic irregular systems it has been conjectured[14] that spectral fluctuations are universally reproduced by appropriate random matrix ensembles, e.g., the Gaussian orthogonal ensemble (GOE) for systems with time-reversal symmetry, giving for $P(S)$ a Wigner distribution.[6,7] This is confirmed by several numerical investigations[6,14–24] as well as theoretical arguments.[25] A recently published semiclassical theory on the Δ_3 statistic[26] for both regular and irregular systems agrees with these results, namely Poisson spectrum and random matrix prediction, respectively.

Recently, special attention has been paid to systems that classically show a transition between the two limiting cases of totally regular and chaotic behavior as a parameter is varied, e.g., the coupling strength or energy.[19–24] For intermediate systems the classical phase space has a complicated structure, consisting for two degrees of freedom of infinitely many distinct regions filled with regular or irregular trajectories, respectively.[1] For more than two degrees of freedom all irregular regions are connected due to Arnold diffusion.[1] It has been argued by Percival[5] that in the semiclassical limit a spectrum should consist of regular and irregular parts that are associated with the classical regular and irregular regions in phase space. Assuming that regular and irregular regions yield energy-level sequences with Poisson and Wigner spacing distributions, respectively, and that the whole spectrum is generated by a statistically independent superposition of those sequences, Berry and Robnik[27] obtained semiclassical formulas for $P(S)$ that interpolate between the two limiting distributions.

The most simple *ansatz* then gives a nns distribution associated with a classical phase space divided in one irregular part with Liouville measure $q_{\rm cl}$ and a regular part with $1-q_{\rm cl}$. By a least-squares fit of this function $P(q;S)$ to a level spacing histogram for a given spectrum one obtains a quantum-mechanical value $q_{\rm qm}$ for this parameter. Indeed, numerical calculations have shown that $q_{\rm cl}$ and

q_{qm} are closely related.[21,22] As expected, the quantum system also exhibits a transitional behavior analogous to the classical transition that is reflected in spectral fluctuation properties.[19–24] It is of course possible to use other (more or less *ad hoc*) ways of interpolating between regular and chaotic behavior[19,20,24] in order to parametrize the smooth transition of $P(S)$ from Poisson to Wigner distribution, but these distributions are not directly amenable to a classical interpretation.

In the present study we therefore shall use Berry and Robnik's approach for the description of the nns distribution $P(S)$ and its extension to the Δ_3 statistic. One of our aims here is to explain the discrepancies found between q_{cl} and q_{qm} in view of (nonsemiclassical) quantum effects and details of the classical phase-space structure. Another point of investigation is the sensitivity of different scales of spectral correlation lengths on the underlying classical motion, i.e., do $P(S)$ and Δ_3 correlate to different classical properties?

In order to reveal such effects as clearly as possible, it is advantageous to study systems that classically have scaling properties. This assures, as already emphasized by Berry and Robnik,[27] that the phase-space structure does not depend on energy. For such systems the semiclassical limit $\hbar \to 0$ is equivalent to the high-energy limit $E \to \infty$, thus the convergence to the semiclassical limit can be studied unambiguously. In this limit, spectral fluctuations are energy independent and many levels can be included for the statistical analysis.

In the following we thus shall investigate a system of two quartic oscillators that are coupled via a quartic term in the coordinates,

$$H=\tfrac{1}{2}(p_x^2+p_y^2+x^4+y^4)-kx^2y^2 . \tag{1}$$

The potential energy is a homogeneous function of the coordinates, implying that apart from scaling the classical motion is independent of energy.[28] Choosing quartic oscillators also avoids the nongeneric properties of harmonic oscillators.[13] Classical calculations for this Hamiltonian, performed by Meyer,[29] show that the chaotic fraction q_{cl} of phase space increases from zero to one if the coupling parameter k, Eq. (1), increases from zero to 0.6.

II. NUMERICAL DETAILS

To obtain quantum energy levels, we expand H, Eq. (1), with $\hbar=1$ in a suitable basis set. For a correct statistical analysis of the level sequence it is important to treat each symmetry class separately, since the corresponding submatrices are independent. In our case H has C_{4v} symmetry, leading to four one-dimensional irreducible representations A_1, A_2, B_1, B_2 and one two-dimensional E representation. For reasons of consistency we did not consider the latter one. Using a basis of symmetry-adapted linear combinations of harmonic-oscillator functions with frequency ω, four submatrices have been diagonalized for each coupling parameter k, Eq. (1) (see Ref. 30 for further details). All basis functions up to a given zeroth-order energy were included; the resulting matrices are banded. Because of the variational principle all eigenvalues of the truncated matrix are upper bounds to the corresponding exact energy levels and so the harmonic frequency ω was chosen such that the trace of this matrix is minimal. This choice of ω is always possible, because the matrix elements of the kinetic, viz., potential, energy are proportional to different powers of ω. For small matrix dimensions we have tested numerically that this procedure yields a maximum number of converged eigenvalues. By the method of Givens rotations[31] the matrices were transformed to tridiagonal form that was subsequently diagonalized by a standard routine.[32] As a criterium for convergence we required level spacings to be accurate within 1%. Like other authors[24] we have found that spectral properties change very rapidly as soon as this limit is exceeded.

We performed calculations for values of $k=0.12$, 0.2, 0.3, 0.4, and 0.6. For $k=0.2$ (intermediate coupling) a dimension of 5476 was used and by comparison with smaller matrices we considered ≈ 2500 eigenvalues to be converged. Each diagonalization required about six hours on an IBM 3081D computer. For all other coupling parameters matrices of dimension 4032 were used [≈ 2.5 h of CPU (central processor unit) time]. For $k=0.6$ (strong coupling) we found only ≈ 850 levels to be converged. For the remaining values of k this number was estimated accordingly. After having checked that spectral properties are essentially independent of the symmetry class, we averaged all statistical measures over the four independent level sequences to obtain results which are statistically more significant.

Before performing statistical analysis one has to remove the secular behavior of the spectral density of the level sequence $\{E_n\}$. In general, this unfolding can be done by using the scaled sequence $\{\mathscr{E}_n = N_{av}(E_n)\}$, where $N_{av}(E)$ is the average number of states below energy E.[6,19] In the case of a classically scaling system with f degrees of freedom, where the potential energy is a homogeneous function of degree s of the coordinates, this can be done easily by

$$\mathscr{E}_n = E_n^{f/2+f/s} . \tag{2}$$

The right-hand side of Eq. (2) gives the semiclassical behavior of $N(E)$, i.e., the number of cells with volume $(2\pi\hbar)^f$ enclosed by the energy shell

$$H(p_1, \ldots, p_f; q_1, \ldots, q_f)=E$$

in phase space. We have checked that in our case ($f=2$, $s=4$) this procedure essentially gives the same results for the subsequent statistical analysis as when unfolding by using cubic spline functions for the smooth behavior of $N(E)$.

III. SHORT-RANGE SPECTRAL CORRELATIONS: $P(S)$

As outlined before, for the analysis of the nns distribution we shall use Berry and Robnik's semiclassical approach. $P(S)$ for the superposition of N independent level sequences is then given by[27]

$$P(S)=\frac{d^2Z(S)}{dS^2}$$
$$Z(S)=\left[\sum_{i=1}^{N}\rho_i\right]^{-1}\prod_{i=1}^{N}\rho_i Z_i(S)\,, \tag{3}$$
$$Z_i(S)=\int_S^\infty d\sigma P_i(\sigma)(\sigma-S)\,.$$

P_i is the nns distribution of the sequence associated with a classical phase-space region of Liouville measure ρ_i. We shall use the simplest form given by

$$P(q;S)=\exp\left[-(1-q)S-\frac{\pi}{4}q^2S^2\right]\times\left[1-q^2+\frac{\pi}{2}q^3S-(1-q)^2R(qS)\right], \tag{4}$$
$$R(Z)=1-\exp(\pi Z^2/4)\operatorname{erfc}(\sqrt{\pi}Z/2)\,,$$

which is generated by superposing a Poisson sequence,

$$P(S)=e^{-S}\,, \tag{5a}$$

and a sequence with Wigner distribution,

$$P(S)=\frac{\pi}{2}Se^{-\pi S^2/4}\,, \tag{5b}$$

with relative weights $1-q$ and q, respectively. $P(q;S)$, Eq. (4), for $q\in[0,1]$ smoothly interpolates between the limiting forms for $P(S)$, Eqs. (5a) and (5b).

Figure 1(a) gives the least-squares-fitted values q_{qm} of the parameter q in $P(q;S)$, Eq. (4), for various level spacing histograms. For each coupling constant k, Eq. (1), several overlapping energy ranges have been analyzed. In Fig. 2 the q_{qm} values obtained from the highest-energy range [cf. Fig. 1(a)] are compared with the classical results for the chaotic phase-space fraction q_{cl}.[29] First, one notes that the fitted values q_{qm} in Fig. 1(a) depend on energy. This dependence, however, decreases with increasing degree of irregularity of the system. In particular, for the smallest nonvanishing coupling parameter $k=0.12$ the system does not seem to have settled to a stationary distribution of $P(S)$ within the energy range under consideration. For this value of k the values for q_{qm} are all far apart from the corresponding classical value of $q_{cl}=0.08$. For the other coupling parameters both values q_{cl} and q_{cm} are closer together.

In order to understand the behavior of the weakly irregular system, i.e., $k=0.12$, we have studied the limiting case of vanishing coupling $k=0$, where the system is separable, hence integrable, and the nns distribution, in the semiclassical limit, should be given by Eq. (5a), i.e., $q_{qm}=0$. The spectrum can be easily obtained by a one-dimensional calculation and a subsequent combination of the levels. Thus far more eigenvalues than in the nonseparable case $k\neq 0$ can be generated. Figure 1(b) shows the resulting values q_{qm} for fitting the distribution $P(q;S)$, Eq. (4), to level spacing histograms obtained from several energy ranges. At lower energies, q_{qm} is quite large and there is very slow convergence to the expected limit $q_{qm}=0$. For $q<0.1$ the distribution $P(q;S)$, Eq. (4), looks very close to a Poisson distribution, but since the number of levels included per histogram in the corresponding energy range was very large ($\approx 2\times 10^4$), the deviations from the semiclassical limit are statistically significant. In particular, for small level spacings S we observed deviations from exponential behavior; cf. Ref. 33 for similar observations.

In light of these results we assume that the nearly integrable system, $k=0.12$, is still far from the semiclassical limit within the numerically accessible energy range. This explains the unexpected large values of q_{qm}. A more detailed discussion will be given in Sec. V.

We consider now the opposite case of strong coupling, $k=0.6$, where the corresponding classical system is total-

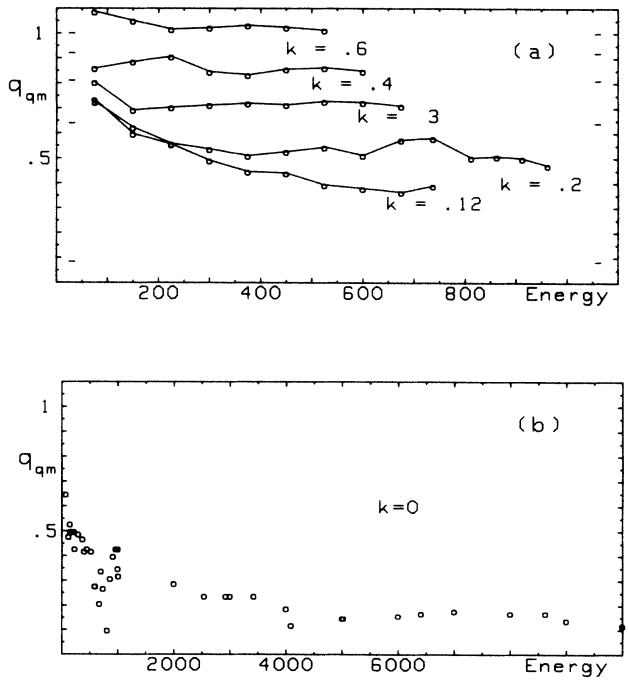

FIG. 1. Fitted values q_{qm}. (a) For energy intervals of width $\Delta E=150$ for $E\leq 675$ and $\Delta E=125$ otherwise. The number of levels per interval varies from ≈ 500 to 1500 (all four nondegenerate symmetry classes are included). (b) For the integrable system, Eq. (1), with $k=0$; also see text.

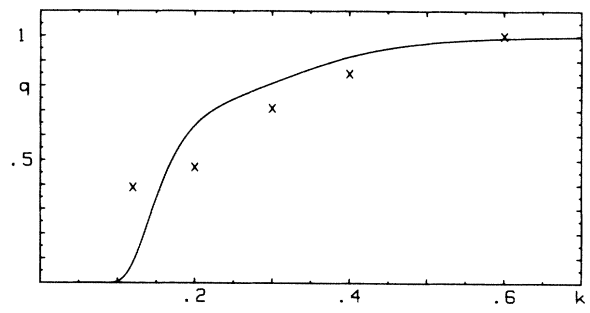

FIG. 2. Classical irregular fraction q_{cl} with respect to the coupling parameter k, Eq. (1), taken from Ref. 29 (solid line) and quantal values q_{qm} for the highest converged energy range, cf. Fig. 1(a).

ly chaotic, i.e., no regular trajectories could be detected numerically.[29] The fitted values q_{qm} for all energy ranges of the quantal spectrum are very close to one ($q_{qm}=1.09,\ldots,1.02$). These unphysically large values are due to statistical fluctuations; a χ^2 analysis shows excellent agreement with the Wigner distribution, Eq. (5b). The system thus, for $P(S)$, exhibits the spectral behavior of the GOE. In contrast to the weak-coupling case, the nns distribution here appears to be translational invariant with respect to energy, i.e., $P(S)$ almost immediately settles to its limiting form.

So far we have discussed the limiting cases of nearly integrable and totally chaotic systems. Figure 2 shows the values q_{qm} of the highest-energy range [cf. Fig. 1(a)] and the classical irregular fractions q_{cl} as functions of the coupling strength k. In the transition region of intermediate coupling the quantal values q_{qm} follow the trend of the classical curve $q_{cl}(k)$, but are generally below it. As already noted and conjectured by other authors,[22,24] this is most probably due to the details of the classical phase-space structure. For two-dimensional systems the irregular part of phase space consists of infinitely many irregular regions.[1] However, only those of significant measure have to be considered; levels deriving from the remaining regions having negligible spectral density.[27] For $P(S)$, then, one has to superpose a regular and several independent irregular sequences. For a given total irregular fraction q the resulting nns distribution tends to a Poisson spectrum as the number of irregular sequences increases. Thus it is obvious that fitting the simple distribution $P(q;S)$ Eq. (4), will give values $q_{qm}<q_{cl}$.

In order to study this in more detail, Fig. 3(a) shows a level spacing histogram for $k=0.2$. For this system, classical computations have shown the irregular phase-space region to consist mainly of three parts with Liouville measures $\rho_1=0.27$ and $\rho_2=\rho_3=0.185$, adding up to a total irregular fraction $q_{cl}=0.64$.[29] Also shown are the nns distributions $P(q_{qm};S)$ Eq. (4), with the fitted value $q_{qm}=0.50$ (solid line); $P(q_{cl};S)$, $q_{cl}=0.64$ (dotted line); as well as $P(S)=P(\rho_1,\rho_2,\rho_3;S)\equiv\bar{P}(S)$ generated by Eq. (3) when using the classically detected three irregular regions (dashed line). Obviously, the level spacing histogram is not described by $P(q_{cl};S)$. For $S>0.5$ (in units of mean level spacing) the histogram is very well approximated by $\bar{P}(S)$, but for smaller S there are substantial deviations. The fitted distribution $P(q_{qm};S)$ lies between the classical curves, trying to match small- and large-S behavior. Similar observations have been made by other authors.[23,24]

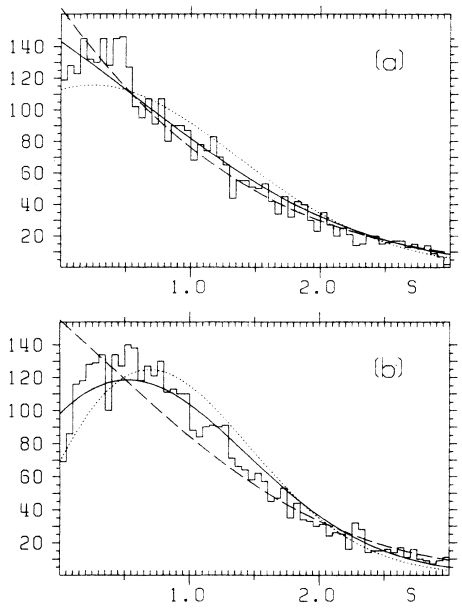

FIG. 3. (a) Level spacing histogram for $k=0.2$ and energy range $700\leq E\leq 1000$, containing ≈ 3600 levels (four symmetry classes). Solid line, $P(q_{qm};S)$, $q_{qm}=0.50$; dotted line, $P(q_{cl};S)$, $q_{cl}=0.64$; dashed line, $\bar{P}(S)$, $\rho_1=0.27$, $\rho_2=\rho_3=0.185$; also see text. (b) Same as (a) with $k=0.3$, $300\leq E\leq 700$, ≈ 4000 levels, $q_{qm}=0.71$, and $q_{cl}=0.81$; also see text.

Figure 3(b) shows an analogous plot for $k=0.3$. Classical computations for this system[29] gave a total irregular fraction $q_{cl}=0.81$, but did not reveal a clearly visible structure of the chaotic region in phase space. For reasons of simplicity we thus assumed the same relative partitioning of the irregular fraction as for $k=0.2$. The curves $P(q_{qm};S)$, $q_{qm}=0.71$, and $P(q_{cl};S)$ are more similar in shape than in Fig. 3(a). $\bar{P}(S)$ completely fails to account for the small-S part of the histogram, although for larger level spacings S it reproduces quite well the observed behavior; small systematic deviations may be due to the above assumption of the Liouville measures entering $\bar{P}(S)$.

There is the general trend that $P(q_{qm};S)$ and $P(q_{cl};S)$ tend to come closer for increasing irregular fraction q_{cl} (cf. Fig. 2). This can be understood by the observation that for increasing coupling strength k the frontiers between distinct irregular regions form an ever more complicated interwoven structure.[29] Thus the effective coarse graining that is imposed on quantal calculations by the finite value of $\hbar$ washes out such fine-scale structures. So effectively will the quantum system "see" only the gross features of phase space, and only in the semiclassical limit as $\hbar\to 0$, increasingly finer details will manifest themselves in the quantum behavior. Equivalently, this may be characterized by quantum tunneling through dynamical barriers which separate the distinct classical irregular regions.

From these arguments one can conclude that the simple nns distribution $P(q;S)$, Eq. (4), is a suitable means to detect quantal manifestations of classical chaos, although there is no exact correspondence between the classical irregular fraction q_{cl} and the fitted quantal value q_{qm}. To summarize briefly, as is for q_{cl} in the classical case, the behavior of the parameter q_{qm} indicates a smooth transition from regularity to irregularity for the quantal system. Deviations between the classical and quantal parameters q_{cl} and q_{qm}, respectively, for small values of q_{cl} can be explained by the slow convergence of the regular spectrum to the semiclassical limit. For larger values of q_{cl}, deviations are due to the partitioning of the irregular phase-space fraction, although this influence is reduced by quantum coarse graining. There remains the question of why level spacing histograms for larger spacings are better approximated by semiclassical predictions than for smaller spacings. This problem will be discussed in Sec. V.

IV. LONG-RANGE SPECTRAL CORRELATIONS: Δ_3 STATISTIC

Besides the distribution of level spacings, the Δ_3 statistic is another well-established measure for spectral fluctuation properties. Given the staircase $N(\mathscr{E})$ (for the unfolded level sequence), i.e., the number of levels below energy $\mathscr{E}$, it is defined as[9]

$$\Delta_3(\mathscr{E};L)=\frac{1}{L}\min_{A,B}\left\{\int_{\mathscr{E}}^{\mathscr{E}+L}[N(\mathscr{E}')-A\mathscr{E}'-B]^2 d\mathscr{E}'\right\}. \tag{6}$$

$\Delta_3(\mathscr{E};L)$ is the least-squares deviation of $N(\mathscr{E})$ from the best straight line fitting it over an interval $[\mathscr{E},\mathscr{E}+L]$. Thus it measures spectral long-range correlations over distances L. Δ_3 is also referred to as spectral rigidity or stiffness. The ensemble average $\bar{\Delta}_3(L)$, i.e., $\Delta_3(\mathscr{E};L)$ averaged over a suitable energy range (see below for details), for an uncorrelated Poisson spectrum $[P(S)=\exp(-S)]$ is given by[6]

$$\bar{\Delta}_3(L)=L/15\ . \tag{7a}$$

This statistic was at first introduced in random matrix theory, where for the GOE, for large L, it is approximately given by[9]

$$\bar{\Delta}_3(L)=\frac{1}{\pi^2}\ln L-0.007\ , \tag{7b}$$

with L in units of mean level spacing. In actual calculations we have used the exact GOE form of $\bar{\Delta}_3(L)$; see Ref. 34, Eq. (4). This behavior of $\bar{\Delta}_3(L)$ has been found in several investigations of experimental[8,34] and numerical[14,18,20,24] data, where also the nns distribution was described by GOE predictions.

The observed universality of the Δ_3 statistic has recently been explained by Berry[26] using a semiclassical theory for $\bar{\Delta}_3(L)$. In particular, for $L\ll L_{\max}$, he essentially verified Eqs. (7a) and (7b) for classically regular systems and chaotic systems with time-reversal symmetry, respectively. For $L\gg L_{\max}$, $\bar{\Delta}_3(L)$ is shown to saturate at a nonuniversal value. The spectral correlation length $L_{\max}$ in units of mean level spacing is given by

$$L_{\max}=2\pi\hbar\frac{\langle d\rangle}{T_{\min}}\ , \tag{8}$$

where $\langle d\rangle$ is the semiclassical mean level density or reciprocal mean level spacing and $T_{\min}$ is the period of the shortest classical closed orbit. Especially for regular systems, the saturation of $\bar{\Delta}_3(L)$ has been observed by several authors.[20,23,24,33] In that case a simple interpretation of this phenomenon can be given as follows. Each energy level of an integrable system via semiclassical quantization is characterized by quantum numbers $n_1,\ldots,n_f$ (f degrees of freedom) corresponding to the values of the f integrals of motion. The whole spectrum can be generated by superposition of level sequences where only one quantum number at a time is varied. For a given energy interval thus only a finite number of sequences will contribute. Varying, e.g., the quantum number n_i, for large n_i the level spacings of this sequence are given by $\hbar\omega_i$, where ω_i is the corresponding classical orbital frequency. Assuming for simplicity that in this energy range all frequencies ω_i, $i=1,\ldots f$, are locally constant, the sequence of level spacings of the superposed sequence in this range will repeat itself after an energy interval $\hbar\omega_{\max}=\hbar\max\{\omega_i\}$. In units of mean level spacing $\langle d\rangle^{-1}$ this argument reproduces Eq. (8). So the spectral pattern essentially repeats itself after $\Delta E=L_{\max}\langle d\rangle^{-1}$ and additional spectral correlations appear beyond distances $L>L_{\max}$, which explains the saturation of $\bar{\Delta}_3(L)$.

Our results for $\bar{\Delta}_3(L)$ for various energy ranges and coupling constants k of the spectrum of the Hamiltonian, Eq. (1), are shown in Figs. 4 and 5. For each energy range $[\mathscr{E},\mathscr{E}+\Delta\mathscr{E}]$ we calculated $\Delta_3(\mathscr{E}',L)$ for 250 overlapping intervals $[\mathscr{E}',\mathscr{E}'+L]\subset[\mathscr{E},\mathscr{E}+\Delta\mathscr{E}]$ in order to obtain the mean value $\bar{\Delta}_3(L)$.[35] For $k\neq 0$ the average subsequently was taken over the four different symmetry classes. In the figures are also shown the Poisson prediction, Eq. (7a), and the exact GOE behavior of $\bar{\Delta}_3(L)$, as well as the values of $L_{\max}$ (crosses), Eq. (8), with $T_{\min}$ at energy E being given by

$$T_{\min}=4\int_0^{(2E)^{1/4}}\frac{dq}{\sqrt{2E-q^4}}=(2E)^{-1/4}\Gamma^2(\tfrac{1}{4})/\sqrt{2\pi}\ , \tag{9}$$

where Γ denotes the usual gamma function. Figures 4(a) and 4(b) show the regular ($k=0$) and totally chaotic ($k=0.6$) systems, respectively. As expected, in both cases $\bar{\Delta}_3(L)$ for small L follows the predicted Poisson and GOE

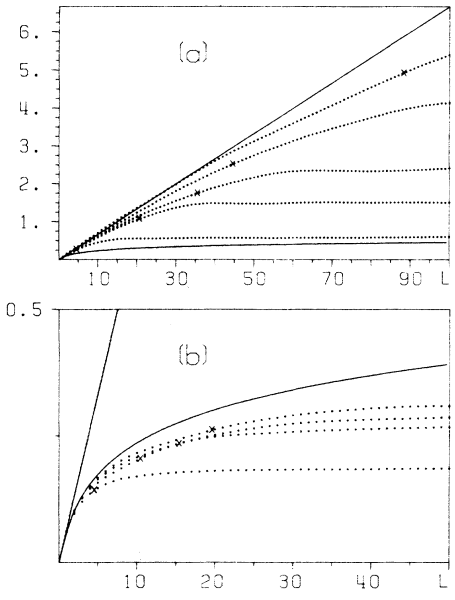

FIG. 4. (a) $\bar{\Delta}_3(L)$ for $k=0$. Solid lines are $L/15$ (diagonal) and GOE prediction (Ref. 35). Dots give calculated $\bar{\Delta}_3(L)$ values for energy ranges [0,200], [400,600], [900,1100], [1900,2100], and [4950,5050] from bottom to top. Crosses indicate the corresponding values $L_{\max}$, Eq. (8). L is in units of mean level spacing. (b) Same as (a) for $k=0.6$ and energy ranges [0,150], [150,300], [300,450], and [450,600].

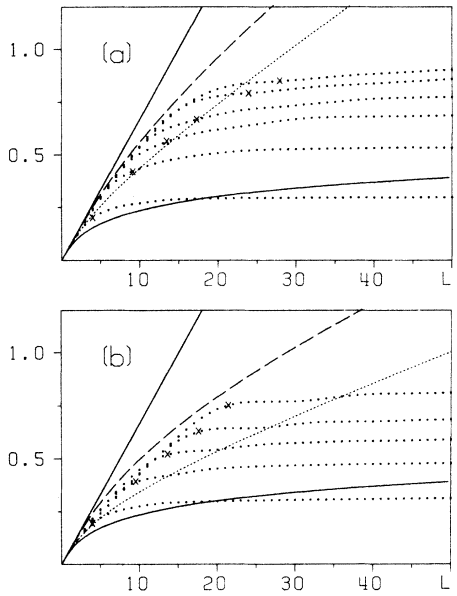

FIG. 5. (a) Same as Fig. 4 for $k=0.2$ and energy ranges [0,150], [150,300], [300,450], [450,600], [750,875], and [950,1050]. Dotted line, semiclassical prediction with one irregular fraction q_{cl}; dashed line, same with three irregular fractions; see text. (b) Same as (a) for $k=0.3$ and energy ranges [0,150], [150,300], [300,450], [450,600], and [600,750]; also see text.

behavior, respectively, and for larger L saturation occurs. The theoretical values L_{max} indeed give the transition region between small-L universal behavior and the large-L nonuniversal saturation regime.

Figures 5(a) and 5(b) represent the intermediate systems $k=0.2$ and 0.3, respectively. The $\bar{\Delta}_3(L)$ values for small L lie between the two limiting curves for Poisson and GOE spectra. Along the same lines of reasoning as for the nns distribution in Sec. III, as already proposed in Ref. 23, it is natural to assume that $\bar{\Delta}_3(L)$ can be calculated via superposition of independent regular and irregular spectral sequences. The result for superposing n sequences with weights ρ_i, $\sum_{i=1}^{n}\rho_i=1$, is given by[36]

$$\bar{\Delta}_3(L)=\sum_{i=1}^{n}\bar{\Delta}_3^{(i)}(\rho_i L)\ , \tag{10}$$

where it is assumed that $\bar{\Delta}_3^{(i)}(L)$ for each sequence i is (locally) independent of energy. The additivity of $\bar{\Delta}_3(L)$ also follows approximately from semiclassical theory.[17] The dotted line in Fig. 5(a) gives Eq. (10) with the classical results $\rho_1=1-q_{cl}$, $\rho_2=q_{cl}=0.64$ and $\bar{\Delta}_3^{(1)},\bar{\Delta}_3^{(2)}$ given by Eqs. (7a) and (7b), respectively. The dashed line also includes the partitioning of the irregular phase space into three parts, cf. Fig. 3(a). Obviously, for small values of L, this latter line gives a remarkably good description of $\bar{\Delta}_3(L)$ as calculated from the spectrum of H, Eq. (1). Crosses again show the semiclassical values of L_{max}, Eq. (8), indicating the region of departure from the universal behavior.

In Fig. 5(b) the corresponding lines are shown for the system with the coupling strength $k=0.3$. The Liouville measure of the classical irregular phase-space fraction is now $q_{cl}=0.81$. Again the observed behavior of $\bar{\Delta}_3(L)$ cannot be reproduced assuming only one classical irregular phase-space region. As already done before in Fig. 3(b), we therefore use the same relative partitioning of the irregular phase-space fraction as for $k=0.2$. The dashed line obtained by this procedure lies fairly close to the actual small-L values of $\bar{\Delta}_3(L)$, deviations of course being due to the assumption of the partitioning used for its construction.

To finish this section we conclude that the classical phase-space structure, in particular the partitioning of the irregular fraction, is quite sensitively reflected by $\bar{\Delta}_3(L)$. The observed additivity of $\Delta_3(L)$ confirms the conjecture that the whole spectrum may be seen as generated by superposition of independent spectral sequences deriving from the separate classical regular and irregular phase-space regions. The large-L saturation of $\bar{\Delta}_3(L)$ can be understood semiclassically as explained above.

V. DISCUSSION

The present investigation gives a further confirmation that the classical transition from regular to irregular motion is reflected by an analogous transition of statistical properties of the corresponding quantum energy-level sequence. In particular, for the system, Eq. (1), we have found that the nns distribution $P(S)$ and the Δ_3 statistic both indicate that in the semiclassical limit there is a transition from an uncorrelated spectrum (Poisson statistic) to a spectrum described by an ensemble of random matrices, namely the GOE. In this limit it is assumed that the whole spectrum is generated by statistically independent superposition of level sequences deriving from separate regular, viz., chaotic, regions of phase space. Systematic deviations from this picture due to quantum effects are found especially for $P(S)$ (Sec. III). In particular, we have found that for small level spacings $S<S_0\approx 1$ the nns distribution $P(S)$ is better represented by neglecting the partitioning of the irregular part in phase space. For larger spacings $S>S_0$, however, this partitioning seems to become important, and in Sec. IV the partitioning was shown to be reflected quite sensitively by $\bar{\Delta}_3(L)$. Thus genuine quantum effects only appear in short-range spectral correlations $S<S_0$, whereas long-range correlations as measured by $P(S)$, $S>S_0$, and by $\bar{\Delta}_3(L)$ agree with semiclassical theory.

These findings can be explained by recognizing that long- and short-range correlations are connected via the uncertainty relation $\Delta E\Delta t\approx\hbar$ with (classical) short- and long-time behavior, respectively. More rigorously, this can be shown using the periodic-orbit expansion, which gives the spectral density as a sum over all classical closed orbits and thus links different scales of spectral resolution with different classical time scales.[26,37,38] A given wave function can semiclassically be associated with a classical phase-space distribution and this connection remains valid for small times during quantal and classical time evolution generated by the Hamilton operator and corresponding Hamilton function, respectively.[37] This association, however, breaks down for longer time scales. Thus the quantum system for small times is essentially mimicked by the classical time evolution and semiclassical con-

siderations are valid, consequently also applying to long-range spectral correlations. For longer times the wave function will spread and thus the system, due to the finite value of $\hbar$, will not be sensitive to finer structures of phase space, leading, e.g., to tunneling through dynamical barriers which classically separate different phase-space regions. As a consequence, there will effectively be only one (or generally very few) irregular region, with $P(S)$ being closer to the simple form $P(q;S)$, Eq. (4). In addition, the interaction between levels deriving from sequences associated with different phase-space regions will lead to level repulsion, i.e., to very small values of $P(S)$ for small $S<S_1$, e.g., for $S_1\approx 0.1$, [cf. Fig. 3(b)]. We found this repulsion to be restricted to increasingly smaller level spacings for increasing energy. This effect will particularly influence the regular spectrum, for which, in the semiclassical limit, the nns distribution $P(S)$ has its maximum at $S=0$. It is thus plausible that the irregular spectrum converges faster to its limiting form, which shows level repulsion, $P(0)=0$, as observed in Sec. III. From the above line of reasoning it becomes clear that in the semiclassical limit, i.e., as $\hbar\to 0$, the limiting correlation lengths S_0,S_1 for validity of semiclassical theory will go to zero. In other words, the semiclassical limit for spectral fluctuations is attained by restricting nonsemiclassical quantum effects to increasingly smaller correlation lengths.

The arguments and results presented here as well as the already-mentioned numerical and theoretical studies strongly suggest that the kind of behavior of spectral fluctuations reported here is typical for a wide class of Hamiltonian systems. In order to obtain a better understanding of this question, we have compared nns distribution properties of several different Hamiltonian systems. In Fig. 6 we compare the convergence to the semiclassical (Poisson) limit for two integrable systems, measured by the fitted parameter $q_{\rm qm}$ of $P(q;S)$, Eq. (4). Circles represent the Hamiltonian, Eq. (1), with $k=0$ [cf. Fig. 1(b)], and crosses the incommensurable rectangular billard, with energy levels $E_{\rm min}=\alpha m^2+n^2$, $\alpha=\pi/3$. The latter system recently has been studied by Casati and Chirikov.[33] Since for scaling systems the limit $E\to\infty$ for fixed $\hbar$ is equivalent to $\hbar\to 0$ for fixed energy E, the abscissa is given in units of $\hbar$. For both systems the value of $\hbar$ corresponding to the 100th energy level E_{100} was fixed to 1. The effective $\hbar$ for energy E is then

$$\hbar(E)=(E/E_{100})^{-(1/2+1/s)}, \tag{11}$$

s being the degree of homogeneity of the potential-energy function, cf. Eq. (2). For the billard system, s is set to infinity. For the calculation of the nns histograms, intervals of length $0.2\hbar$ centered around $\hbar$ were taken. In this representation both systems show a very similar behavior of the fitted values $q_{\rm qm}$ with respect to $\hbar$ (Fig. 6). In particular, in both cases there is very slow convergence to the Poisson limit. Even in the energy range above the 50 000th energy level, which corresponds to values of $\ln\hbar<-3.11$ (cf. figure caption), the nns distribution still shows significant deviations from the expected Poisson distribution.

A hint in order to understand this similar behavior may be given by the following consideration. As already explained in Sec. IV the spectrum of a classically integrable system can be generated by superposition of level sequences where only one quantum number at a time is varied. The number of sequences $n(E)$ contributing to a given spectral range around energy E for a system with two degrees of freedom is approximately given by the number of levels $N_1(E)$ of the one-dimensional system and thus we have [cf. Eq. (2)]

$$n(E)\approx N_1(E)\propto\hbar^{-1}. \tag{12}$$

The Poisson limit is attained as the number of sequences $n(E)$ becomes infinitely large and the sequences effectively become mutually uncorrelated. The slow convergence to this limit may be due to the fact that the individual level sequences to be superposed are not truly independent. In addition, the weights of the contributing sequences differ considerably since their level density decreases with increasing energy. Thus many more individual sequences are required to generate Poisson-like spectra as when, e.g., superposing sequences with equal weights.

To complete the discussion, Fig. 7 compares the fitted values $q_{\rm qm}$ with the corresponding classical irregular fractions $q_{\rm cl}$ for three systems showing a transition from regular to irregular behavior as a parameter is varied. Circles

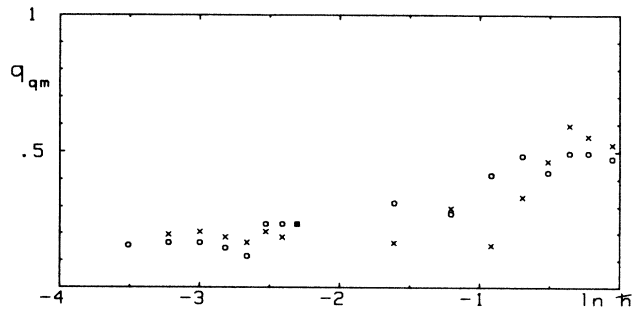

FIG. 6. Fitted values $q_{\rm qm}$ with respect to $\hbar$. Circles refer to the Hamiltonian, Eq. (1), with $k=0$; crosses refer to rectangular billard; see text. The number of levels below energy $E(\hbar)$ is approximately given by $N=100\hbar^{-2}$.

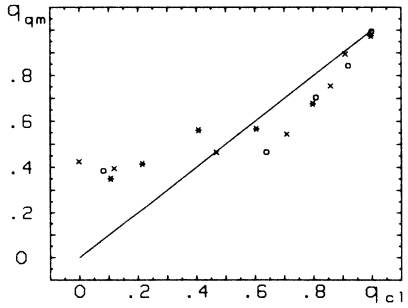

FIG. 7. Comparison of quantal values $q_{\rm qm}$ and corresponding classical irregular fractions $q_{\rm cl}$. The line $q_{\rm qm}=q_{\rm cl}$ is indicated. Circles, crosses, and stars represent different systems; see text.

derive from the system, Eq. (1) (cf. Fig. 2), crosses are adapted from an investigation of a (scaling) billard system with irregularly curved boundaries,[22] and stars are taken from Ref. 21, where two coupled harmonic oscillators have been studied. The latter system has no scaling property with respect to energy. All three systems show similar deviations from the line $q_{qm}=q_{cl}$. In particular, for small q_{cl} the quantal values q_{qm} lie above that line, which can be explained by the slow convergence to the semiclassical limit for nearly regular sequences. For intermediate irregular phase-space fractions q_{cl} this trend reverses and the values q_{qm} become smaller than q_{cl}. As already discussed, this is due to the partitioning of the irregular fraction, which leads to more Poisson-like spectra. A plot like Fig. 7 will of course depend on how good the semiclassical regime is attained, but due to similar computational restrictions all three systems will approximately have reached a similar degree of convergence.

There is thus strong evidence that spectral fluctuations for a probably wide class of Hamiltonian systems show a universal behavior that is connected with the classical phase-space structure. Semiclassical theories for $P(S)$ in the regular case[13] and for the Δ_3 statistic for both regular and irregular systems[26] are an important step towards an understanding of this universality. The present work shows that the nns distribution and the Δ_3 statistic in actual computations, where the semiclassical limit is not fully reached, respond differently to the underlying classical motion. The deviations from the expected limit, however, are systematic and can be understood by a simple picture for the quantum effects. An interesting question for future investigations will be the extension to three degrees of freedom, in particular how Arnold diffusion is reflected in quantum spectra by $P(S)$ and $\overline{\Delta}_3(L)$.

ACKNOWLEDGMENTS

This work was financially supported by the Deutsche Forschungsgemeinschaft (Bonn, West Germany).

[1]A. J. Lichtenberg and M. A. Liebermann, *Regular and Stochastic Motion* (Springer, New York, 1983).
[2]M. J. Davis, E. B. Stechel, and E. Heller, Chem. Phys. Lett. **76**, 21 (1980); E. J. Heller and M. J. Davis, J. Phys. Chem. **86**, 2118 (1982); N. Moiseyev and A. Peres, J. Chem. Phys. **79**, 5945 (1983).
[3]M. Shapiro and G. Goelman, Phys. Rev. Lett. **53**, 1714 (1984).
[4]A. Peres, Phys. Rev. Lett. **53**, 1711 (1984); M. Feingold, N. Moiseyev, and A. Peres, Chem. Phys. Lett. **117**, 344 (1985).
[5]I. C. Percival, J. Phys. B **6**, L229 (1973).
[6]O. Bohigas and M.-J. Giannoni, in *Mathematical and Computational Methods in Nuclear Physics*, Vol. 209 of *Lecture Notes in Physics*, edited by J. S. Dehesa, J. M. G. Gomez, and A. Polls (Springer, New York, 1984).
[7]*Statistical Theories of Spectra: Fluctuations*, edited by C. E. Porter (Academic, New York, 1965).
[8]T. A. Brody, J. Flores, J. B. French, P. A. Mello, A. Pandey, and S. S. M. Wong, Rev. Mod. Phys. **53**, 385 (1981).
[9]F. J. Dyson and M. L. Mehta, J. Math. Phys. **4**, 701 (1963) (reprinted in Ref. 7).
[10]H. S. Camarda and P. D. Georgopulos, Phys. Rev. Lett. **50**, 492 (1983).
[11]E. Haller, H. Köppel, and L. S. Cederbaum, Chem. Phys. Lett. **101**, 215 (1983); V. Buch, R. B. Gerber, and M. A. Ratner, J. Chem. Phys. **76**, 5397 (1982).
[12]In the following we shall use the terms "regular" and "irregular," or "chaotic," always with respect to the corresponding classical system.
[13]M. V. Berry and M. Tabor, Proc. R. Soc. London, Ser. A **356**, 375 (1977).
[14]O. Bohigas, M. J. Giannoni, and C. Schmit, Phys. Rev. Lett. **52**, 1 (1984).
[15]S. W. McDonald and A. N. Kaufman, Phys. Rev. Lett. **42**, 1189 (1979).
[16]M. V. Berry, Ann. Phys. (N.Y.) **131**, 163 (1981).
[17]G. Casati, F. Valz-Griz, and I. Guarneri, Lett. Nuovo Cimento **28**, 279 (1980).
[18]O. Bohigas, M. J. Giannoni, and C. Schmit, J. Phys. (Paris) Lett. **45**, L1015 (1984).
[19]E. Haller, H. Köppel, and L. S. Cederbaum, Phys. Rev. Lett. **52**, 1665 (1984).
[20]T. H. Seligman, J. J. M. Verbaarschot, and M. R. Zirnbauer, Phys. Rev. Lett. **53**, 215 (1984).
[21]H.-D. Meyer, E. Haller, H. Köppel, and L. S. Cederbaum, J. Phys. A **17**, L831 (1984).
[22]T. Ishikawa and T. Yukawa, Phys. Rev. Lett. **54**, 1617 (1985).
[23]T. H. Seligman and J. J. M. Verbaarschot, J. Phys. A **18**, 2227 (1985).
[24]T. H. Seligman, J. J. M. Verbaarschot, and M. R. Zirnbauer, J. Phys. A **18**, 2751 (1985).
[25]P. Pechukas, Phys. Rev. Lett. **51**, 943 (1983); T. Yukawa, *ibid.* **54**, 1883 (1985).
[26]M. V. Berry, Proc. R. Soc. London, Ser. A **400**, 229 (1985).
[27]M. V. Berry and M. Robnik, J. Phys. A **17**, 2413 (1984).
[28]L. D. Landau and E. M. Lifshitz, *Mechanics*, 2nd ed. (Pergamon, Oxford, 1969).
[29]H.-D. Meyer, J. Chem. Phys. **84**, 3147 (1986).
[30]R. A. Pullen and A. R. Edmonds, J. Phys. A **14**, L477 (1981).
[31]J. H. Wilkinson and C. Reinsch, *Linear Algebra* (Springer, New York, 1970), Chap. II/8.
[32]Reference 31, Chap. II/3.
[33]G. Casati and B. V. Chirikov, Phys. Rev. Lett. **54**, 1350 (1985); M. Feingold, *ibid.* **55**, 2626 (1985).
[34]R. U. Haq, A. Pandey, and O. Bohigas, Phys. Rev. Lett. **48**, 1086 (1982).
[35]For $\Delta_3(E,L)$ we used a simple closed formula derived in O. Bohigas and M. J. Giannoni, Ann. Phys. (N.Y.) **84**, 393 (1975).
[36]A. Pandey, Ann. Phys. (N.Y.) **119**, 170 (1979).
[37]M. V. Berry, in *Chaotic Behaviour of Deterministic Systems*, edited by R. H. G. Helleman and G. Joos (North-Holland, Amsterdam, 1983), and references therein.
[38]M. V. Berry, in *The Wave-Particle Dualism*, edited by S. Diner, D. Fargue, G. Lochak, and F. Selleri (Reidel, Dordrecht, 1984), and references therein.